# QCD viscosity to entropy density ratio in the hadronic phase

Jiunn-Wei Chen, Yen-Han Li, Yen-Fu Liu, and Eiji Nakano

*Department of Physics and Center for Theoretical Sciences, National Taiwan University, Taipei 10617, Taiwan*

(Received 20 April 2007; revised manuscript received 22 September 2007; published 14 December 2007)

The shear viscosity $\eta$ of QCD in the hadronic phase is computed by the coupled Boltzmann equations of pions and nucleons in low temperatures and low baryon-number densities. The $\eta$ to entropy density ratio $\eta/s$ maps out the nuclear gas-liquid phase transition by forming a valley tracing the phase transition line in the temperature-chemical potential plane. When the phase transition turns into a crossover, the $\eta/s$ valley gradually disappears. We suspect the general feature for a first-order phase transition is that $\eta/s$ has a discontinuity in the bottom of the $\eta/s$ valley. The discontinuity coincides with the phase transition line and ends at the critical point. Beyond the critical point, a smooth $\eta/s$ valley is seen. However, the valley could disappear further away from the critical point. The $\eta/s$ measurements might provide an alternative to identify the critical points.

DOI: 10.1103/PhysRevD.76.114011 PACS numbers: 12.38.Mh, 51.20.+d

## I. INTRODUCTION

Shear viscosity $\eta$ is a transport coefficient which has recently been attracting lots of attention. It characterizes how strongly particles interact and move collectively in a many-body system. In general, the stronger the interparticle interaction, the smaller the shear viscosity. It is conjectured [1] that, no matter how strong the interparticle interaction is, the shear viscosity to entropy density $s$ ratio has a minimum bound $1/4\pi$, i.e., $\eta/s \geq 1/4\pi$ in any system. The bound was motivated by the uncertainty principle and the observation that $\eta/s = 1/4\pi$ for a large class of strongly interacting quantum field theories whose dual descriptions in string theory involve black holes in anti–de Sitter space [2–5]. In Ref. [1], supporting evidence of the conjecture was given for matters like $H_2O$, He, and N. Their $\eta/s$ curves reach their minima near the gas-liquid phase transitions with the bound well satisfied. Recently, $\eta/s$ close to the minimum bound was found in relativistic heavy ion collisions [6–8] (and in lattice simulations of a gluon plasma [9]) just above the deconfinement temperature $T_c$ ($\sim 170$ MeV at zero baryon density [10]). This suggests the quark gluon plasma (QGP) is strongly interacting at this temperature, which is quite different from the traditional picture of weakly interacting QGP.[1] (However, see Ref. [19] for a different interpretation.) Also, $\eta/s$ close to the minimum bound was found in cold fermionic atoms in the infinite scattering length limit [20]. A relation between $\eta/s$ and the jet quenching parameter in QGP was proposed in Ref. [21].

In Refs. [22,23], it was found that $\eta/s$ of QCD in the confinement and deconfinement phases is qualitatively different. When $T < T_c$ (the confinement phase), $\eta/s$ is monotonically decreasing in $T$ because the system is dominated by Goldstone bosons which interact more weakly at lower $T$. When $T > T_c$ (the deconfinement phase), $\eta/s$ is monotonically increasing in $T$ because the interaction between quarks and gluons is weaker at higher $T$ due to asymptotic freedom. It makes perfect sense to have the phase transition from the point of view of preserving the $\eta/s$ minimum bound. This is because if the qualitative behavior of $\eta/s$ is not changed by a phase transition (or crossover), then the bound could be violated. One concludes that the minimum or valley of the $\eta/s$ curve lies in the vicinity of $T_c$ [the extrapolation of the low (high) temperature $\eta/s$ curve sets a upper (lower) bound on $T_c$] [23]. This behavior is also seen in the $H_2O$, He, and N systems. It was further noticed that below the critical pressure, a cusp appears at the minimum of $\eta/s$, which coincides with the critical temperatures [22].

In Ref. [24], it is argued that a universal minimum bound on $\eta/s$ should not exist. The counterexample given is a system of mesons made by heavy quarks and light antiquarks. Since $s$ scales linearly with the number of heavy quark flavor $N_f$ and $\eta$ is insensitive to $N_f$, the $\eta/s \geq 1/4\pi$ bound could be violated in some special large $N_f$ limit. However, this system is metastable. As far as the qualitative relation between $T_c$ and the valley of $\eta/s$ is concerned, it does not matter if the minimum bound of $\eta/s$ is $1/4\pi$ or 0. As long as there is a lower bound, the monotonic behavior of $\eta/s$ will be affected by the bound.

In this manuscript, we extend the discussion of the $\eta/s$ of QCD in the confinement phase at zero baryon chemical potential $\mu$ [23] to finite $\mu$ and study its relation to the QCD phase diagram. String theory methods give $\eta/s = 1/4\pi$ for $\mathcal{N} = 4$ supersymmetric theories with finite R-charge density, suggesting the minimum bound is independent of $\mu$. For QCD, the fermion sign problem (the fermion determinant is not positive definite) makes the current lattice QCD methods inapplicable in the low $T$ and finite $\mu$ regime. An alternative is to use effective field theory (EFT). Reliable results using EFT in hadronic degrees of freedom can be obtained when both $T$ and $\mu$ are small. At higher $\mu$ (with $|k_F a| \gg 1$, where $k_F$ denotes the Fermi momentum and $a$ is the nucleon-nucleon scattering length)

[1] See also [11–13]. For discussions of the possible microscopic structure of such a state, see [14–18]

 

the problem becomes nonperturbative in coupling and mean-field treatments are not sufficient. (It is essentially the same type of problem as in cold fermionic atoms near the infinite scattering length limit.) Nonperturbative computations of the EFT on the lattice are free from the fermion sign problem at the leading order (LO) with only nonderivative contact interactions [25]. But this theory is suitable only in low $T$ and low density systems. For the nuclear matter problem, the inclusion of one pion exchange will reintroduce the sign problem. However, the sign problem is claimed to be mild and lattice simulations are still possible [26]. The computation of $\eta$ using lattice nuclear EFT has not been carried out before. Although $\eta$ is associated with real time response to perturbations, it can be reconstructed through the spectral function computed on the Euclidean lattice [9,27].

As an exploratory work, we compute $\eta$ using coupled Boltzmann equations for a system of a pion $\pi$ and nucleon $N$ while the entropy $s$ is computed in equilibrium with particle interactions neglected. Higher resonances such as kaons and delta resonances are neglected because their masses are much larger than the range of $T$ and $\mu$ explored here. The delta resonances, however, could couple to $\pi N$ strongly. But putting delta in the intermediate states in $\pi N$ scattering only changes $\eta/s$ by less than 8%. Thus, although this approach will not give accurate $\eta/s$ in the regime dominated by near threshold $NN$ interaction, for most of the regime we are exploring, our result should be robust.

## II. LINEARIZED BOLTZMANN EQUATION FOR LOW ENERGY QCD

We are interested in the hadronic phase of QCD with nonzero baryon-number chemical potential $\mu$. For reference, a schematic QCD phase diagram from a recent review [28] is shown in Fig. 1. The detailed structures of the quark matter phases are still unclear. When $\mu \ll m_N$ ( $= 938$ MeV, the nucleon mass) the nucleon population is exponentially suppressed. The dominant degrees of freedom are the lightest hadrons—the pions. The pion mass $m_\pi (= 139$ MeV) is much lighter than the mass of the next lightest hadron—the kaon whose mass is 495 MeV. Given that $T_c$ is only $\lesssim 170$ MeV, it is sufficient to just consider the pions in the calculation of thermodynamical quantities and transport coefficients for $T \ll T_c$. When $m_N - \mu < m_\pi$, the nucleon population is no longer suppressed compared with the pion. We will limit ourselves to the low $T$ and low $\mu$ region where only $\pi$ and $N$ are important degrees of freedom.

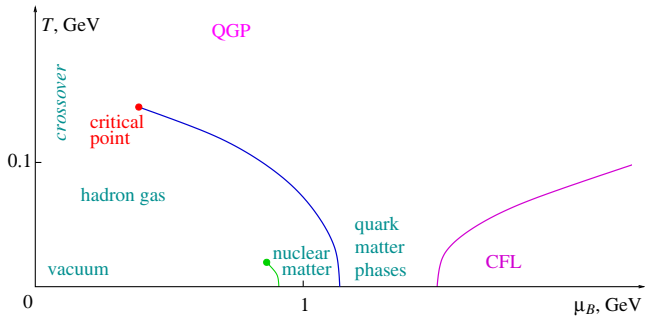


FIG. 1 (color online). A semiquantitative sketch of the QCD phase diagram [28] courtesy of M. Stephanov.

The shear viscosity of a system is defined by the Kubo formula

$$\eta = -\frac{1}{5}\int_{-\infty}^{0} dt' \int_{-\infty}^{t'} dt \int d\mathbf{x}^3 \langle [T^{ij}(0), T^{ij}(\mathbf{x}, t)] \rangle, \quad (1)$$

with $T^{ij}$ the spatial part of the off-diagonal energy momentum tensor. The Kubo formula involves an infinite number of diagrams at the LO even in the weak coupling $\phi^4$ theory [29]. However, it is proven that the summation of LO diagrams in a weak coupling $\phi^4$ theory is equivalent to solving the linearized Boltzmann equation with temperature dependent particle masses and scattering amplitudes [29]. We will assume the equivalence between the Kubo formula and the Boltzmann equation still hold in our $\pi N$ system. Later we will check whether the mean free path is still much larger than the range of interaction. This is a requirement to apply the Boltzmann equation which makes use of semiclassical descriptions of particles with definite position, energy, and momentum except during brief collisions.

In the Boltzmann equation of our $\pi N$ system, the evolution of the isospin averaged $\pi$ and $N$ distribution functions $f^{\pi,N} = f^{\pi,N}(\mathbf{x}, \mathbf{p}, t) \equiv f_p^{\pi,N}(x)$ (functions of space, time, and momentum) are caused by interparticle $\pi\pi$, $\pi N$, and $NN$) collisions,

$$\begin{aligned} \frac{p^\mu}{E_p^\pi}\partial_\mu f_p^\pi(x) = \frac{g_\pi}{2}\int_{123} d\Gamma^{\pi\pi}_{12;3p}\{&f_1^\pi f_2^\pi F_3^\pi F_p^\pi \\ &- F_1^\pi F_2^\pi f_3^\pi f_p^\pi\} \\ &+ g_N \int_{123} d\Gamma^{\pi N}_{12;3p}\{f_1^N f_2^\pi F_3^N F_p^\pi \\ &- F_1^N F_2^\pi f_3^N f_p^\pi\}, \end{aligned} \quad (2)$$

$$\begin{aligned} \frac{p^\mu}{E_p^N}\partial_\mu f_p^N(x) = \frac{g_N}{2}\int_{123} d\Gamma^{NN}_{12;3p}\{&f_1^N f_2^N F_3^N F_p^N \\ &- F_1^N F_2^N f_3^N f_p^N\} \\ &+ g_\pi \int_{123} d\Gamma^{\pi N}_{12;3p}\{f_1^\pi f_2^N F_3^\pi F_p^N \\ &- F_1^\pi F_2^N f_3^\pi f_p^N\}, \end{aligned} \quad (3)$$

where $F_i^{\pi(N)} \equiv 1 \pm f_i^{\pi(N)}$, $E_p^{\pi(N)} = \sqrt{\mathbf{p}^2 + m^2_{\pi(N)}}$, and the spin and isospin degeneracy factors $g_\pi = 3$ and $g_N = 4$.

$$d\Gamma^{\pi N}_{12;3p} \equiv |\mathcal{T}_{\pi N}|^2 \frac{(2\pi)^4 \delta^4(k_1 + k_2 - k_3 - p)}{2^4 E_1^N E_2^\pi E_3^N E_p^\pi} \prod_{i=1}^{3} \frac{d^3\mathbf{k}_i}{(2\pi)^3}, \tag{4}$$

where $\mathcal{T}_{\pi N}$ is the $\pi N$ scattering amplitude with momenta $1,\ 2 \to 3,\ p$. The $\pi\pi$ and $NN$ weighted integration measures are given analogously. We use the LO chiral perturbation theory ($\chi$PT) [30–33] result for the isospin averaged $\pi\pi$ scattering amplitude in terms of Mandelstam variables ($s$, $t$, and $u$)

$$|\mathcal{T}_{\pi\pi}|^2 = \frac{1}{9 f_\pi^4}[21 m_\pi^4 + 9 s^2 - 24 m_\pi^2 s + 3(t-u)^2], \tag{5}$$

where $f_\pi = 93$ MeV. The isospin averaged $NN$ scattering amplitudes are described by effective range expansion [34]. In the center of mass (CM) frame

$$|\mathcal{T}_{NN}|^2 = 3(4\pi m_N)^2 \Big[ \Big| -\frac{1}{a_1} + \frac{1}{2} r_1 p^2 - ip \Big|^{-2} + \Big| -\frac{1}{a_3} + \frac{1}{2} r_3 p^2 - ip \Big|^{-2} \Big], \tag{6}$$

where $p$ is the magnitude of the nucleon momentum in the CM frame and $a_{1(3)}$ and $r_{1(3)}$ are the spin singlet (triplet) scattering length and effective range, respectively. $a_1 = -17.9$,[2] $a_3 = 5.42$, $r_1 = 2.77$, and $r_3 = 1.76$, all in units of fm. Note that near the threshold ($p = 0$), $|\mathcal{T}_{NN}|^2$ is proportional to $a_1^2 + a_3^2$ which is greatly enhanced by the large scattering lengths. The interaction is smaller away from the threshold.

The $\pi N$ scattering $[\pi(q_1)N(p_1) \to \pi(q_2)N(p_2)]$ amplitude is also given by $\chi$PT [35]. It is known that the delta resonance is heavier than the nucleon by $\Delta = 294$ MeV, so its density is negligible compared with the nucleon in the range of $T$ and $\mu$ that we are considering. However, it could contribute to the $\pi N$ scattering intermediate states through the tails of thermal distributions. Thus, we also include it to study the effects of baryon resonances. In the CM frame

$$\begin{aligned}
|\mathcal{T}_{\pi N}|^2 &= \frac{1}{2}(E_N + m_N)^2[|g_+|^2 + 2|g_-|^2 + q^4 \sin^2\theta(|h_+|^2 + 2|h_-|^2)], \\
g_+ &= -\frac{2 g_{\pi N\Delta}^2}{9 f_\pi^2}\Big(\frac{1}{\omega - \Delta - i\Gamma/2} - \frac{1}{\omega + \Delta - i\Gamma/2}\Big)(2\omega^2 - 2m_\pi^2 + t), \\
g_- &= \frac{g_{\pi N\Delta}^2}{9 f_\pi^2}\Big(\frac{1}{\omega - \Delta - i\Gamma/2} + \frac{1}{\omega + \Delta - i\Gamma/2}\Big)(2\omega^2 - 2m_\pi^2 + t) - \frac{g_A^2}{f_\pi^2}\frac{1}{4\omega}(2\omega^2 - 2m_\pi^2 + t) + \frac{\omega}{2 f_\pi^2}, \\
h_+ &= \frac{2 g_{\pi N\Delta}^2}{9 f_\pi^2}\Big(\frac{1}{\omega - \Delta - i\Gamma/2} + \frac{1}{\omega + \Delta - i\Gamma/2}\Big) - \frac{g_A^2}{f_\pi^2}\frac{1}{2\omega}, \\
h_- &= -\frac{g_{\pi N\Delta}^2}{9 f_\pi^2}\Big(\frac{1}{\omega - \Delta - i\Gamma/2} - \frac{1}{\omega + \Delta - i\Gamma/2}\Big) - \frac{g_A^2}{f_\pi^2}\frac{1}{2\omega},
\end{aligned} \tag{7}$$

where $g_{\pi N\Delta} = 1.05$ is the $\pi - N - \Delta$ coupling, $g_A = 1.26$ is the $\pi N$ coupling constant, $\Gamma = 120$ MeV is the delta width, $E_N$ is the nucleon energy, $q$ is the magnitude of pion momentum, $\theta$ is the angle between $q_1$ and $q_2$, and $\omega$ is the pion energy. Formally the delta width $\Gamma$ is a higher-order effect in $\chi$PT. This power counting works fine in the region below the delta resonance threshold. However, in our case, $\omega$ can be greater than $\Delta$ in the thermal distributions. Thus, we have included $\Gamma$ in the LO expression as a regulator. The thermal corrections for $\pi\pi$, $\pi N$ scattering amplitudes and particle masses are higher order in $\chi$PT. The $T$ dependence in $NN$ scattering amplitude is also small at low $T$. Because the thermal correction for the inverse scattering length scales as $T$ which is much smaller than the thermal momentum $\sim\sqrt{m_N T}$, it can be neglected.

[2]We have used the isospin averaged scattering length defined as $a_1^2 = (a_{nn}^2 + a_{np}^2 + a_{pp}^2)/3$.

In local thermal equilibrium, the distribution functions are $\bar{f}_p^\pi(x) = (e^{\beta(x)V_\mu(x)p^\mu} - 1)^{-1}$, where $\beta(x)$ is the inverse temperature, $V^\mu(x)$ is the four velocity of the fluid at the space-time point $x$, and $\tilde{p}^\mu = (E_p^N - \mu, \mathbf{p})$ in the $\mathbf{V}(x) = 0$ frame. A small deviation of $f_p$ from local equilibrium can be parametrized as

$$f_p^l(x) = \bar{f}_p^l(x)[1 - \bar{F}_p^l(x)\chi_p^l(x)], \qquad l = \pi, N, \tag{8}$$

with $\bar{F}_i^{\pi(N)} \equiv 1 \pm \bar{f}_i^{\pi(N)}$. The energy momentum tensor is

$$T_{\mu\nu}(x) = \int \frac{\mathrm{d}^3\mathbf{p}}{(2\pi)^3} p_\mu p_\nu \Big[\frac{g_\pi f_p^\pi(x)}{E_p^\pi} + \frac{g_N f_p^N(x)}{E_p^N}\Big]. \tag{9}$$

We will choose the frame with zero fluid velocity $\mathbf{V}(x) = 0$ at the point $x$. This implies $\partial_\nu V^0 = 0$ after taking a derivative on $V_\mu(x)V^\mu(x) = 1$. Furthermore, the conservation law at equilibrium $\partial_\mu T^{\mu\nu}|_{\chi_p = 0} = 0$ allows us to replace

$\partial_t\beta(x)$ and $\partial_t\mathbf{V}(x)$ by terms proportional to $\nabla\cdot\mathbf{V}(x)$ and $\nabla\beta(x)$. Thus, to the first order in a derivative expansion, $\chi_p^l(x)$ can be parametrized as

$$\frac{\chi_p^l(x)}{\beta(x)} = A^l(p)\nabla\cdot\mathbf{V}(x) + B_{ij}^l(p) \times\left(\frac{\nabla_i V_j(x)+\nabla_j V_i(x)}{2} - \frac{\delta_{ij}}{3}\nabla\cdot\mathbf{V}(x)\right), \tag{10}$$
$$B_{ij}^l(p) \equiv B^l(p)\left(\hat{p}_i\hat{p}_j - \frac{1}{3}\delta_{ij}\right),$$

where $i$ and $j$ are spatial indices. $A$ and $B$ are functions of $x$ and $p$. However, we have suppressed the $x$ dependence.

Substituting Eq. (10) into the Boltzmann equation Eq. (2), one obtains a linearized equation for $B^\pi$:

$$\begin{aligned}\left(p_ip_j - \frac{1}{3}\delta_{ij}\mathbf{p}^2\right) &= \frac{g_\pi E_p^\pi}{2}\int_{123} d\Gamma_{12;3p}^{\pi\pi}\bar{F}_1^\pi\bar{F}_2^\pi\bar{f}_3^\pi(\bar{F}_p^\pi)^{-1}[B_{ij}^\pi(p)+B_{ij}^\pi(k_3)-B_{ij}^\pi(k_2)-B_{ij}^\pi(k_1)]\\ &\quad + g_N E_p^\pi\int_{123} d\Gamma_{12;3p}^{\pi N}\bar{F}_1^\pi\bar{F}_2^N\bar{f}_3^N(\bar{F}_p^\pi)^{-1}[B_{ij}^\pi(p)-B_{ij}^\pi(k_1)+B_{ij}^N(k_3)-B_{ij}^N(k_2)]\\ &\equiv g_\pi G_{ij}^{\pi\pi}[B^\pi] + g_N G_{1ij}^{\pi N}[B^\pi] + g_N G_{2ij}^{\pi N}[B^N].\end{aligned} \tag{11}$$

The analogous equation for $B^N$ is obtained by replacing $\pi\leftrightarrow N$ on the right-hand side of the above equation. There are two other integral equations involving $A^l(p)\nabla\cdot\mathbf{V}(x)$ which are related to the bulk viscosity $\zeta$. They will not be treated in this work.

In fluid dynamics the energy-momentum tensor at equilibrium depends on pressure $P(x)$ and energy density $\epsilon(x)$ as $T_{\mu\nu}^{(0)}(x) = \{P(x)+\epsilon(x)\}V_\mu(x)V_\nu(x) - P(x)\delta_{\mu\nu}$. A small deviation away from equilibrium gives an additional contribution to $T_{\mu\nu} = T_{\mu\nu}^{(0)} + \delta T_{\mu\nu}$, whose spatial components define the shear and bulk viscosity,

$$\delta T_{ij} = \zeta\delta_{ij}\nabla\cdot\mathbf{V}(x) - \eta\left(\nabla_iV_j(x)+\nabla_jV_i(x) - \frac{2}{3}\delta_{ij}\nabla\cdot\mathbf{V}(x)\right). \tag{12}$$

Comparing the above definition with Eqs. (9) and (10), we obtain

$$\begin{aligned}\eta &= g_\pi L^\pi[B^\pi] + g_N L^N[B^N],\ L^l[B^l]\\ &= \frac{\beta}{15}\int\frac{d^3\mathbf{p}\mathbf{p}^2}{(2\pi)^3E_p^k}\bar{f}_p^l\bar{F}_p^lB^l(p).\end{aligned} \tag{13}$$

Now one sees immediately that if all the $\pi\pi$, $\pi N$, and $NN$ scattering cross sections are reduced by a factor $\lambda$, then Eq. (11) implies the $B^l$ functions will be $\lambda$ times larger. Then by Eq. (13), $\eta$ will be $\lambda$ times larger as well. This is the nonperturbative feature of the Boltzmann equation. It gives a divergent $\eta$ for a noninteracting theory.

Contracting both sides of Eq. (11) by $(\hat{p}_i\hat{p}_j - \delta_{ij}/3)$ and applying it to Eq. (13) yields

$$\begin{aligned}\eta &= \frac{\beta}{10}\int\frac{d^3\mathbf{p}}{(2\pi)^3}\frac{g_\pi}{E_p^\pi}\bar{f}_p^\pi\bar{F}_p^\pi B_{ij}^\pi(p)\\ &\quad\times\{g_\pi G_{ij}^{\pi\pi}[B^\pi] + g_N G_{1ij}^{\pi N}[B^\pi] + g_N G_{2ij}^{\pi N}[B^N]\}\\ &\quad + [\pi\leftrightarrow N]\\ &\equiv g_\pi^2\langle B_\pi|G^{\pi\pi}[B_\pi]\rangle + g_\pi g_N\{\langle B_\pi|G_1^{\pi N}[B_\pi]\rangle\\ &\quad + \langle B_\pi|G_2^{\pi N}[B_N]\rangle\} + [\pi\leftrightarrow N].\end{aligned} \tag{14}$$

To compute $\eta$, one can just solve $B^{\pi(N)}(p)$ from Eq. (11). But here we follow the approach outlined in Ref. [36,37] to assume that $B^{\pi(N)}(p)$ is a smooth function which can be expanded using a specific set of orthogonal polynomials:

$$\begin{aligned}B^l(p) &= |\mathbf{p}|^y\sum_{r=0}^\infty b_r^l B_l^{(r)}(z(p))\\ &\equiv \sum_{r=0}^\infty b_r^l\tilde{B}_l^{(r)}(z(p)), \qquad l=\pi,N,\end{aligned} \tag{15}$$

where $B_l^{(r)}(z)$ is a polynomial up to $z^r$ and $b_r^l$ is its coefficient. The overall factor $|\mathbf{p}|^y$ will be chosen by trial and error to get the fastest convergence. We find that using $y=1.89$ and $z(p)=|\mathbf{p}|$, the series converges rather rapidly. The orthogonality condition

$$\frac{\beta}{15}\int\frac{d^3\mathbf{p}}{(2\pi)^3}\frac{|\mathbf{p}|^{2+y}}{E_p^l}\bar{f}_p^l\bar{F}_p^lB_l^{(r)}(z)B_l^{(s)}(z) = L_l^{(r)}\delta_{r,s} \tag{16}$$

can be used to construct the $B_l^{(r)}(z)$ polynomials up to normalization constants. For simplicity, we will choose

$$B_l^{(0)}(z) = 1. \tag{17}$$

With this setup, Eqs. (13) and (17) yield

$$\eta = \sum_r [g_\pi b_r^\pi L_\pi^{(r)} + g_N b_r^N L_N^{(r)}]\delta_{0,r}, \tag{18}$$

while Eq. (14) yields

$$\begin{aligned}\eta = \sum_{r,s=0}^{\infty} & g_\pi b_r^\pi \{ g_\pi b_s^\pi \langle \tilde{B}_\pi^{(r)} | G^{\pi\pi}[\tilde{B}_\pi^{(s)}] \rangle \\ & + g_N [ b_s^\pi \langle \tilde{B}_\pi^{(r)} | G_1^{\pi N}[\tilde{B}_\pi^{(s)}] \rangle + b_s^N \langle \tilde{B}_\pi^{(r)} | G_2^{\pi N}[\tilde{B}_N^{(s)}] \rangle ] \} \\ & + [\pi \leftrightarrow N].\end{aligned} \tag{19}$$

The $b_r^\pi$'s and $b_r^N$'s are functions of $\mu$ and $T$. In general they are independent of each other. Thus the above two equations yield

$$\delta_{r,0} \begin{pmatrix} L_\pi^{(0)} \\ L_N^{(0)} \end{pmatrix} = \sum_s \begin{pmatrix} \pi\pi^{rs} & \pi N^{rs} \\ N\pi^{rs} & NN^{rs} \end{pmatrix} \begin{pmatrix} g_\pi b_s^\pi \\ g_N b_s^N \end{pmatrix}, \tag{20}$$

where the matrix elements are given by

$$\begin{aligned} \pi\pi^{rs} &= \langle \tilde{B}_\pi^{(r)} | G^{\pi\pi}[\tilde{B}_\pi^{(s)}] \rangle + \frac{g_N}{g_\pi} \langle \tilde{B}_\pi^{(r)} | G_1^{\pi N}[\tilde{B}_\pi^{(s)}] \rangle, \\ \pi N^{rs} &= \langle \tilde{B}_\pi^{(r)} | G_2^{\pi N}[\tilde{B}_N^{(s)}] \rangle, \\ NN^{rs} &= \langle \tilde{B}_N^{(r)} | G^{NN}[\tilde{B}_N^{(s)}] \rangle + \frac{g_\pi}{g_N} \langle \tilde{B}_N^{(r)} | G_1^{N\pi}[\tilde{B}_N^{(s)}] \rangle, \\ N\pi^{rs} &= \langle \tilde{B}_N^{(r)} | G_2^{N\pi}[\tilde{B}_\pi^{(s)}] \rangle. \end{aligned} \tag{21}$$

The matrix equation in Eq. (20) allows us to solve for $b_s$ and obtain the shear viscosity. Since the expansion in Eq. (15) converges rapidly, one does not need to keep many terms to solve for $\eta$. If only the $s = 0$ term is kept, then

$$\eta \simeq \begin{pmatrix} L_\pi^{(0)} \\ L_N^{(0)} \end{pmatrix}^T \begin{pmatrix} \pi\pi^{00} & \pi N^{00} \\ N\pi^{00} & NN^{00} \end{pmatrix}^{-1} \begin{pmatrix} L_\pi^{(0)} \\ L_N^{(0)} \end{pmatrix}. \tag{22}$$

The computation of the entropy density $s$ is more straightforward since $s$, unlike $\eta$, does not diverge when particle interactions are neglected. The contributions from $\pi\pi$ and $\pi N$ scattering are perturbative and are higher-order effects in $\chi$PT. The $NN$ contribution is also perturbative at low $\mu$, but it becomes nonperturbative at $\mu \approx m_N$ and low $T$. In this regime, the system is governed by near threshold $NN$ interaction. With that limitation in mind, we compute $s$ in equilibrium with particle interactions neglected:

$$s = -\beta^2 \frac{\partial}{\partial\beta} \frac{g_\pi \log Z_\pi + g_N \log Z_N}{\beta}, \tag{23}$$

where the partition function $Z_{\pi(N)}$ for pions (nucleons) is

$$\frac{\log Z_{\pi(N)}}{\beta} = \mp \frac{1}{\beta} \int \frac{d^3\mathbf{p}}{(2\pi)^3} \log\{1 \mp e^{-\beta \tilde{E}_p^{\pi(N)}}\}, \tag{24}$$

with $\tilde{E}_p^\pi \equiv E_p^\pi$ and $\tilde{E}_p^N \equiv E_p^N - \mu$, up to temperature independent terms.

## III. $\eta/s$ AND THE QCD PHASE DIAGRAM

In Fig. 2, $\eta/s$ as a function of $T$ and $\mu$ is shown as a 3-D plot and a contour plot. Note that at the corner of large $\mu$ and large $T$, the system is no longer in the hadronic phase. Thus, the result should be discarded there. In general $\eta/s$ is decreasing in $T$ except when $\mu \simeq m_N$ and $T < 30$ MeV. (This regime is blown up in Fig. 3 and will be studied later.) There are some interesting structures at larger $\mu$, but $\eta/s$ is $\mu$ independent when $\mu < 500$ MeV. This is because when $\mu \ll m_N$ the nucleons only exist through particle-antiparticle pair creations, thus they are highly suppressed. The $\eta/s$ is determined by the pion gas which is $\mu$ independent. Our result just reproduces the $\mu = 0$ result of Ref. [23] (see [36–39] for earlier results) in this regime.

When $\mu > m_N - m_\pi = 800$ MeV, the nucleon population is no longer suppressed compared with the pion population and when $\mu \gtrsim m_N$, the nucleons become the dominant degrees of freedom. Numerically $\eta/s$ is dominated by the nucleon contributions when $\mu > 800$ MeV. It is decreasing in both $T$ and $\mu$ until $\mu \simeq m_N$. This is

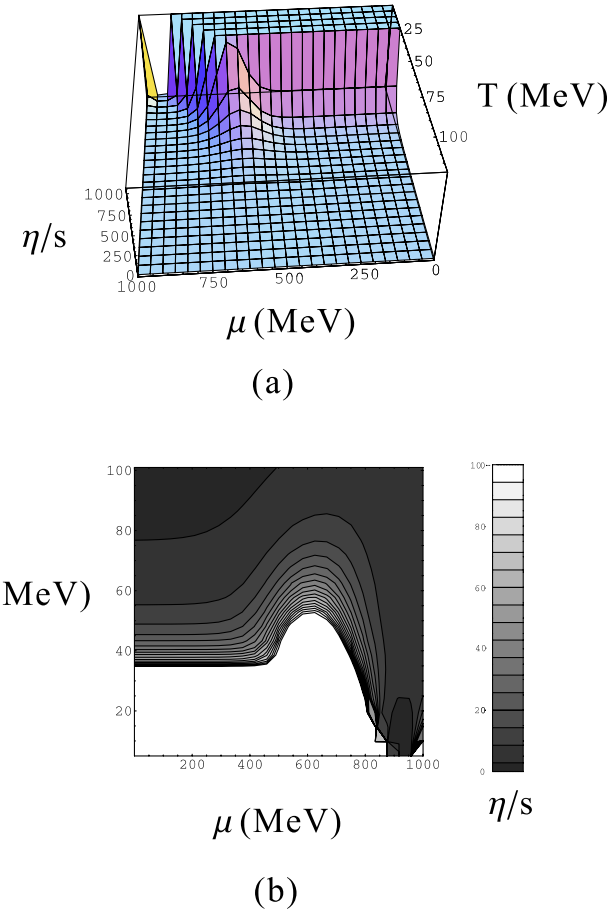


FIG. 2 (color online). $\eta/s$ of QCD as a function of $T$ and $\mu$ shown as a 3-D plot (a) and a contour plot (b). Note that the corner of large $\mu$ and large $T$ should be discarded since it is not in the hadronic phase.

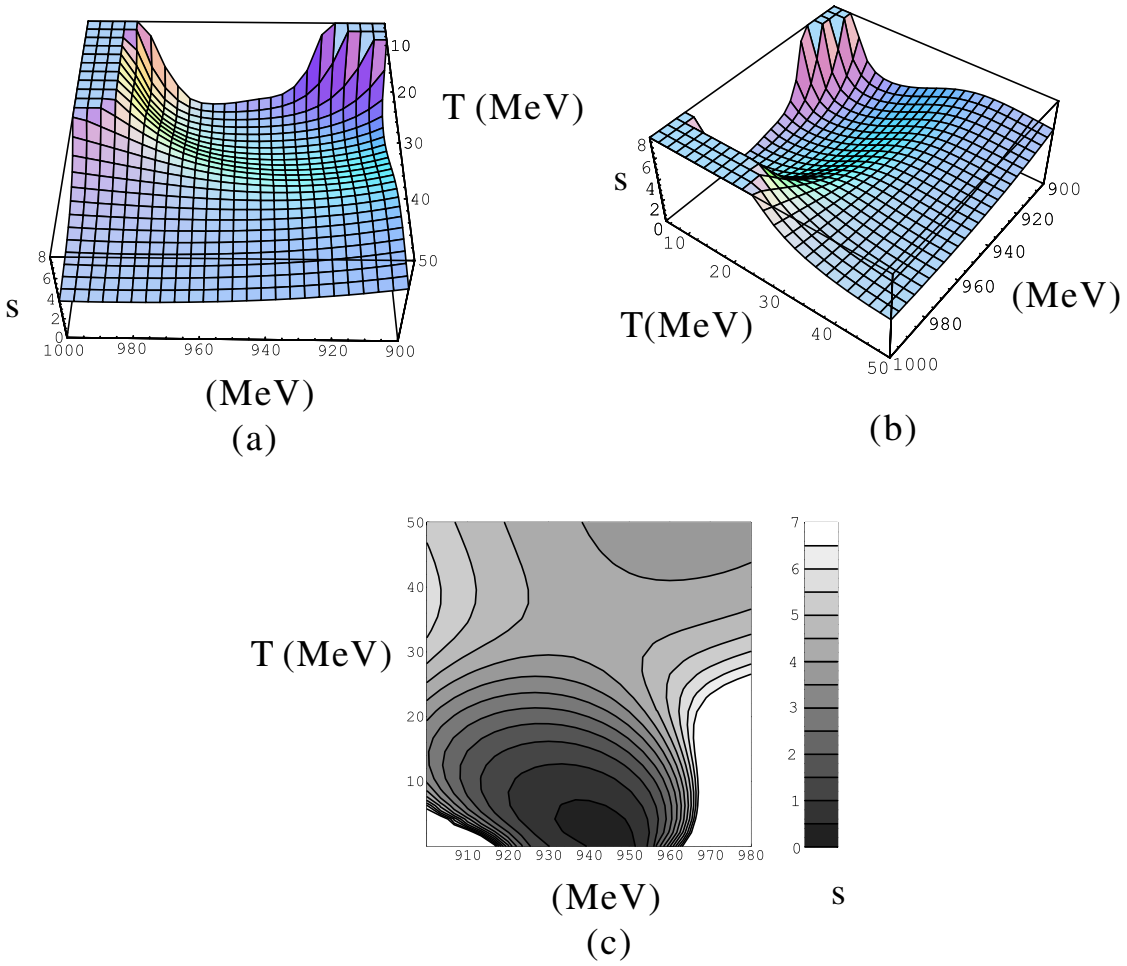


FIG. 3 (color online). $\eta/s$ of QCD near the nuclear gas-liquid phase transition shown as 3-D plots (a) and (b), viewed from different angles, and a contour plot (c). The $\eta/s$ maps out the nuclear gas-liquid phase transition shown in Fig. 1 by forming a valley tracing the nuclear gas-liquid phase transition line in the $T-\mu$ plane. When the phase transition turns into a crossover at larger $T$, the valley also gradually disappears at around 30 MeV. There should be a discontinuity that looks like a fault in the bottom of the $\eta/s$ valley that is not seen in our approximation. The fault would lie on top of the phase transition line and end at the critical point ($T \sim 10$–$15$ MeV in our result). Beyond the critical point, $\eta/s$ turns into a smooth valley. The valley could disappear far away from the critical point. Similar behavior is also seen in water shown in Fig. 4. We suspect these are general features for first-order phase transitions.

because $s$ is increasing in both $T$ and $\mu$ while $\eta$ is getting smaller at higher $\mu$ (larger nucleon population) and lower $T$ (stronger interaction, closer to the interaction threshold). 500–800 MeV in $\mu$ is the transition between the $\pi$ and $N$ dominant regimes. The largest effect of the delta resonance is a 48% increase of $\eta$ at $T \simeq 50$ MeV and $\mu \simeq 600$ MeV. The effect is reduced to be less than 10% outside the 300–800 MeV window in $\mu$.

Now let us focus on the $\mu \simeq m_N$ and $T < 30$ MeV region in the $\eta/s$ plot. Two 3-D plots viewed from different angles are shown in Fig. 3(a) and 3(b)and a contour plot is shown in Fig. 3(c). One clearly sees that $\eta/s$ maps out the nuclear gas-liquid phase transition shown in Fig. 1 by forming a valley tracing the nuclear gas-liquid phase transition line in the $T-\mu$ plane. When the phase transition turns into a crossover at larger $T$, the valley also gradually disappears at around 30 MeV. This result is encouraging.

However, even though the gross features of the phase transition are mapped out by the $\eta/s$ valley nicely, some details are not correct. First, since the density is discontinuous across the first-order phase transition, $\eta$, $s$, and $\eta/s$ are likely to be discontinuous across the phase transition as observed in $H_2O$, He, and N systems in Ref. [22]. This discontinuity, which defines the critical chemical potential $\mu_c$, should lie at the bottom of the $\eta/s$ valley. Second, the position of $\mu_c$ suggested by our result is not correct. Near $T = 0$, one expects $\mu_c \simeq m_N - \langle B \rangle$, where $\langle B \rangle$ is the binding energy per nucleon, but we have $\mu_c > m_N$.

It is quite obvious that our treatment of $s$ is very poor near the phase transition. However, we have not pursued other treatments like the mean-field approximation in this work because it is known that the approximation is insufficient when $|k_F a| \gg 1$. For the same reason, the compu-

tation of $\eta$ using the Boltzmann equation might not be justified near the bottom the valley even though the mean free path is still bigger than the range of potential ( $\sim 1$ fm). However, the valley of $\eta$ is located at $\mu < m_N$ near $T = 0$; thus, it is possible that after reliable $s$ is used, $\mu_c$ for $\eta/s$ will be in the correct position. Furthermore, the regime in Fig. 3 is completely dominated by the nucleon degree of freedom ($\eta/s$ hardly changes with the thermal pions completely ignored). This simplifies the problem significantly and makes the system exhibit universal properties shared by dilute fermionic systems with large scattering lengths such as cold atoms tuned to be near a Feshbach resonance.

As mentioned above, it was observed that below the critical pressure, $\eta/s$ has a discontinuity at the critical temperature for $H_2O$, He, and N, and above the critical pressure, $\eta/s$ has a smooth minimum near the crossover temperature (defined as the temperature where the density changes rapidly) [22]. For QCD at $\mu = 0$, $\eta/s$ also has a valley near the crossover temperature [22,23]. But there is no evidence yet to show the valley is smooth or has a discontinuity.

We suspect $\eta/s$ should be smooth in a crossover and should have a discontinuity across a first-order phase transition. If this is correct, then in a nuclear gas-liquid transition, there should be a discontinuity looking like a fault in the bottom of the $\eta/s$ valley. The fault would lie on top of the phase transition line and end at the critical point where the first-order phase transition turns into a crossover. If we look at Fig. 3(c), we would conclude that the critical point is at $T \sim 10$–$15$ MeV, agreeing with 7–16 MeV from experimental extractions [40–42]. Near the critical point, a smooth $\eta/s$ valley is seen in the crossover (like the confinement-deconfinement crossover of QCD at $\mu = 0$); however, the valley could disappear far away from the critical point. We suspect these are general features of first-order phase transitions. Indeed, this behavior is seen in all the materials with data available in the NIST and CODATA websites [43,44], including Ar, CO, $CO_2$, H, He, $H_2O$, $H_2S$, Kr, N, $NH_3$, Ne, O, and Xe. As an example, $\eta/s$ of water vs. temperature in different pressures is plotted in Fig. 4. Below the critical pressure 22.06 MPa, $\eta/s$ has a discontinuity at the minimum. Above the critical pressure, $\eta/s$ becomes smooth. Its minimum moves toward the large $T$ and large $P$ direction and eventually moves out of the plotted range, such that $\eta/s$ looks like a monotonic function in $T$. Thus, one might use $\eta/s$ measurements to identify the first-order phase transition and the critical point (see Refs. [22,45] for a similar point of view).

Also, for all the materials listed above except CO, the $\eta/s$ has a positive jump across the phase transition line from the gas to the liquid phase as shown in Fig. 4. For CO, the jump is positive at smaller pressure but becomes small and negative at higher pressure. It is interesting to recheck whether CO really is an anomaly. However, even without considering CO, the sign of the $\eta/s$ jump for first-order phase transitions might not be universal, either. For QCD in the limit of a large number of colors, the jump is negative from the low to high temperature phases [22].

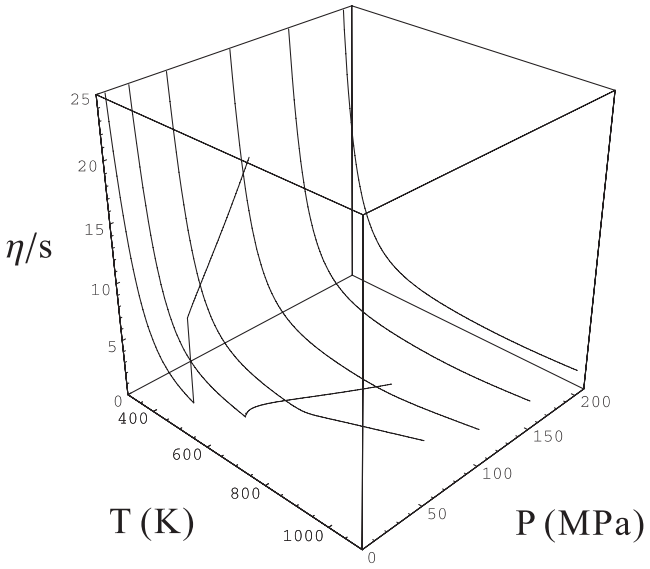


FIG. 4. $\eta/s$ of water vs temperature in different pressures. Below the critical pressure 22.06 MPa, $\eta/s$ has a discontinuity at the minimum. Above the critical pressure, $\eta/s$ becomes smooth. Its minimum moves toward the large $T$ and large $P$ direction and eventually moves out of the plotted range, such that $\eta/s$ looks like a monotonic function in $T$. Similar behaviors are seen in all the materials with data available in [43,44], including Ar, CO, $CO_2$, H, He, $H_2S$, Kr, N, $NH_3$, Ne, O, and Xe.

## IV. CONCLUSION

We have computed the shear viscosity of QCD in the hadronic phase by the coupled Boltzmann equations of pions and nucleons in low temperatures and low baryon-number densities. The ratio $\eta/s$ maps out the nuclear gas-liquid phase transition by forming a valley tracing the phase transition line in the temperature-chemical potential plane. When the phase transition turns into a crossover, the $\eta/s$ valley also gradually disappears. We suspect the general feature for a first-order phase transition is that $\eta/s$ has a discontinuity in the bottom of the $\eta/s$ valley. The discontinuity coincides with the phase transition line and ends at the critical point. Beyond the critical point, a smooth $\eta/s$ valley is seen on the crossover side. However, the valley could disappear far away from the critical point. The $\eta/s$ measurements might provide an alternative to identify the critical points.

## ACKNOWLEDGMENTS

We thank Dick Furnstahl for pointing out Refs. [40–42] to us. This work was supported by the NSC and NCTS of Taiwan, ROC.

[1] P. Kovtun, D. T. Son, and A. O. Starinets, Phys. Rev. Lett. **94**, 111601 (2005).

[2] G. Policastro, D. T. Son, and A. O. Starinets, Phys. Rev. Lett. **87**, 081601 (2001).

[3] G. Policastro, D. T. Son, and A. O. Starinets, J. High Energy Phys. 09 (2002) 043.

[4] C. P. Herzog, J. High Energy Phys. 12 (2002) 026.

[5] A. Buchel and J. T. Liu, Phys. Rev. Lett. **93**, 090602 (2004).

[6] I. Arsene *et al.*, Nucl. Phys. **A757**, 1 (2005); B. B. Back *et al.*, *ibid.* **A757**, 28 (2005); J. Adams *et al.*, *ibid.* **A757**, 102 (2005); K. Adcox *et al.*, *ibid.* **A757**, 184 (2005).

[7] D. Molnar and M. Gyulassy, Nucl. Phys. **A697**, 495 (2002); **A703**, 893(E) (2002).

[8] D. Teaney, Phys. Rev. C **68**, 034913 (2003).

[9] A. Nakamura and S. Sakai, Phys. Rev. Lett. **94**, 072305 (2005).

[10] F. Karsch and E. Laermann, in *Quark-Gluon Plasma 3*, edited by R. C. Hwa and X.-N. Wang (World Scientific, Singapore, 2004), p. 1.

[11] M. Asakawa and T. Hatsuda, Phys. Rev. Lett. **92**, 012001 (2004).

[12] S. Datta, F. Karsch, P. Petreczky, and I. Wetzorke, Phys. Rev. D **69**, 094507 (2004).

[13] T. Umeda, K. Nomura, and H. Matsufuru, Eur. Phys. J. C **39S1**, 9 (2005).

[14] E. V. Shuryak and I. Zahed, Phys. Rev. D **70**, 054507 (2004).

[15] V. Koch, A. Majumder, and J. Randrup, Phys. Rev. Lett. **95**, 182301 (2005).

[16] J. Liao and E. V. Shuryak, Phys. Rev. D **73**, 014509 (2006).

[17] G. E. Brown, C.-H. Lee, M. Rho, and E. V. Shuryak, Nucl. Phys. **A740**, 171 (2004).

[18] G. E. Brown, C.-H. Lee, M. Rho, Nucl. Phys. **A747**, 530 (2005).

[19] M. Asakawa, S. A. Bass, and B. Muller, Phys. Rev. Lett. **96**, 252301 (2006).

[20] T. Schafer, arXiv:cond-mat/0701251.

[21] A. Majumder, B. Muller, and X. N. Wang, Phys. Rev. Lett. **99**, 192301 (2007).

[22] L. P. Csernai, J. I. Kapusta, and L. D. McLerran, Phys. Rev. Lett. **97**, 152303 (2006).

[23] J. W. Chen and E. Nakano, Phys. Lett. B **647**, 371 (2007).

[24] T. D. Cohen, Phys. Rev. Lett. **99**, 021602 (2007).

[25] J. W. Chen and D. B. Kaplan, Phys. Rev. Lett. **92**, 257002 (2004).

[26] B. Borasoy, E. Epelbaum, H. Krebs, D. Lee, and U. G. Meissner, Eur. Phys. J. A **31**, 105 (2007).

[27] F. Karsch and H. W. Wyld, Phys. Rev. D **35**, 2518 (1987).

[28] M. A. Stephanov, Proc. Sci., LAT2006 (2006) 024 [arXiv:hep-lat/0701002].

[29] S. Jeon, Phys. Rev. D **52**, 3591 (1995); S. Jeon and L. Yaffe, Phys. Rev. D **53**, 5799 (1996).

[30] S. Weinberg, Phys. Rev. Lett. **18**, 188 (1967); R. Dashen and M. Weinstein, Phys. Rev. **183**, 1261 (1969); L.-F. Li and H. Pagels, Phys. Rev. Lett. **26**, 1204 (1971); P. Langacker and H. Pagels, Phys. Rev. D **8**, 4595 (1973); S. Weinberg, Physica A (Amsterdam) **96**, 327 (1979); S. Coleman, J. Wess, and B. Zumino, Phys. Rev. **177**, 2239 (1969); C. Callan, S. Coleman, J. Wess, and B. Zumino, Phys. Rev. **177**, 2247 (1969).

[31] J. Gasser and H. Leutwyler, Nucl. Phys. **B250**, 465 (1985); Ann. Phys. (N.Y.) **158**, 142 (1984).

[32] E. Jenkins and A. V. Manohar, Phys. Lett. B **255**, 558 (1991).

[33] V. Bernard, N. Kaiser, and Ulf-G. Meissner, Int. J. Mod. Phys. E **4**, 193 (1995).

[34] H. A. Bethe, Phys. Rev. **76**, 38 (1949); H. A. Bethe and C. Longmire, Phys. Rev. **77**, 647 (1950).

[35] N. Fettes and U. G. Meissner, Nucl. Phys. **A679**, 629 (2001); N. Fettes, U. G. Meissner, and S. Steininger, Nucl. Phys. **A640**, 199 (1998).

[36] A. Dobado and S. N. Santalla, Phys. Rev. D **65**, 096011 (2002).

[37] A. Dobado and F. J. Llanes-Estrada, Phys. Rev. D **69**, 116004 (2004).

[38] D. Davesne, Phys. Rev. C **53**, 3069 (1996).

[39] M. Prakash, M. Prakash, R. Venugopalan, and G. M. Welke, Phys. Rev. Lett. **70**, 1228 (1993); Phys. Rep. **227**, 321 (1993).

[40] J. B. Natowitz *et al.*, Phys. Rev. C **65**, 034618 (2002).

[41] J. B. Elliott *et al.* (EOS Collaboration), Phys. Rev. C **67**, 024609 (2003).

[42] L. G. Moretto, J. B. Elliott, and L. Phair, Phys. Rev. C **72**, 064605 (2005).

[43] E. W. Lemmon, M. O. McLinden, and D. G. Friend, in *NIST Chemistry WebBook*, NIST Standard Reference Database Number 69, edited by P. G. Linstrom and W. G. Mallard (National Institute of Standards and Technology, Gaithersburg, MD, 2003), p. 20899, http://webbook.nist.gov.

[44] J. D. Cox, D. D. Wagman, and V. A. Medvedev, *CODATA Key Values for Thermodynamics* (Hemisphere Publishing Corp., New York, 1989, http://www.codata.org).

[45] R. A. Lacey *et al.*, Phys. Rev. Lett. **98**, 092301 (2007).